Journal of Organometallic Chemistry, 438 (1992) 167–182
Elsevier Sequoia S.A., Lausanne
JOM 22800

Anodic oxidation of the ferrocenyl-derived β-ketophosphine $[Ph_2PCH_2C(O)(\eta^5\text{-}C_5H_4)Fe(\eta^5\text{-}C_5H_5)]$ and of two of its palladium complexes. Ferricinium-mediated oxidation of palladium(II)–phosphine complexes

Alain Louati, Maurice Gross

Laboratoire d'Electrochimie et de Chimie Physique du Corps Solide, U.R.A. au CNRS n°. 405, Université Louis Pasteur, 4 rue Blaise Pascal, 67070 Strasbourg Cedex (France)

Laurent Douce

Laboratoire de Chimie de Coordination, U.R.A. au CNRS n°. 416, Université Louis Pasteur, 4 rue Blaise Pascal, 67070 Strasbourg Cedex (France)

and Dominique Matt

Laboratoire de Chimie Minérale, U.R.A. au CNRS n°. 405, Ecole Européenne des Hautes Etudes des Industries Chimiques de Strasbourg, 1 rue Blaise Pascal, 67008 Strasbourg Cedex (France)

(Received February 6, 1992)

Abstract

The anodic behaviour of the ferrocenyl-derived compounds $[Ph_2PCH_2C(O)(\eta^5\text{-}C_5H_4)Fe(\eta^5\text{-}C_5H_5)]$ (1), $[(o\text{-}C_6H_4CH_2NMe_2)Pd\{Ph_2PCH{=}C(O)(\eta^5\text{-}C_5H_4)Fe(\eta^5\text{-}C_5H_5)\}]$ (2) and $[(o\text{-}C_6H_4CH_2NMe_2)PdCl\{Ph_2PCH_2C(O)(\eta^5\text{-}C_5H_4)Fe(\eta^5\text{-}C_5H_5)\}]$ (3) has been investigated in dichloromethane at a platinum electrode. Voltammetric and coulometric data, and spectral results, indicate that for each compound, the first electron loss corresponding to the oxidation of the ferrocenyl centre triggers an intramolecular electron transfer. In complexes 2 and 3, this results in the formation of transient radical cationic Pd^{III} species whereas for 1 the electron transfer probably leads to a phosphonium cation radial.

Introduction

An organometallic complex containing two or more metal centres in sufficiently close proximity may exhibit, as a consequence of steric and electronic interactions, chemical and physical properties different from those displayed by a mixture of the mononuclear components [1]. Such a synergistic effect is of considerable importance in the search for new physical properties, as well as for enhancing the stoichiometric or catalytic reactivity of metal complexes. Bimetallic systems con-

---

Correspondence to: Dr. A. Louati or Professor M. Gross.

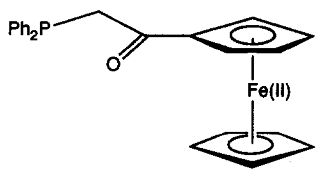

(1)

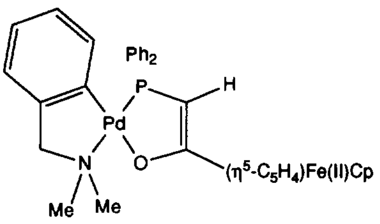

(2)

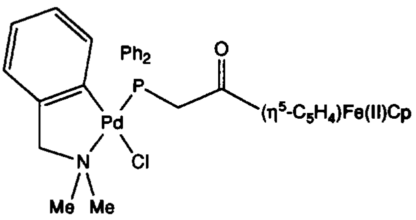

(3)

taining metals with widely differing properties offer not only the possibility of bifunctional activation of an organic substrate but also that of sequential reactions on distinct metal centres. Such complexes could be useful for the activation of feedstock molecules such as carbon monoxide and carbon dioxide under mild conditions. Other bimetallic systems may provide sites for multi-electron redox reactions, enabling the systems to act as electron-storage devices, or allowing electronic communication between the metals [2].

As a part of our studies on ferrocenyl ligands, we have now investigated the electrochemical properties of the phosphine $[Ph_2PCH_2C(O)(\eta^5\text{-}C_5H_4)Fe(\eta^5\text{-}C_5H_5)]$ (**1**) and of two bimetallic complexes containing **1**, namely $[(o\text{-}C_6H_4CH_2NMe_2)Pd\{Ph_2PCH{=}C(O)(\eta^5\text{-}C_5H_4)Fe(\eta^5\text{-}C_5H_5)\}]$ (**2**) and $[(o\text{-}C_6H_4CH_2NMe_2)PdCl\{Ph_2PCH_2C(O)(\eta^5\text{-}C_5H_4)Fe(\eta^5\text{-}C_5H_5)\}]$ (**3**).

Experimental

All experiments were carried out under argon. The β-ketophosphine **1**, and the palladium complexes **2** and **3** were synthesized according to the method previously described [3].

Compound **1** and complexes **2** and **3** are chemically stable in CH_2Cl_2; no change in the electronic absorption spectra nor in the electrochemical characteristics of these molecules was observed after storing them for a few days under argon.

The ^1H and $^{31}P\{^1H\}$ NMR spectra were recorded on a Bruker SY 200 spectrometer. The IR spectra were recorded in the range 4000–400 cm^{-1} on a FT-IR Bruker IFS 66 spectrometer. The UV–visible spectra were recorded on a Shimadzu UV 260 spectrometer. The ESR X-band spectra were recorded on a Bruker ER 420 spectrometer equipped with a cooling system.

Electrochemical measurements were carried out in CH_2Cl_2, purified by distillation over P_2O_5. The supporting electrolyte used for voltammetric methods was tetrabutylammonium perchlorate (TBAP). For the preparative electrolysis, instead of TBAP, we used tetraethylammonium perchlorate (TEAP) which is more easily separated from the reaction mixture. The two electrolytes were purified by recrystallization (from an ethanol/water mixture for TBAP and from methanol for TEAP) and further dried *in vacuo* before use.

Voltammetry at a rotating disk electrode was performed with a Bruker E 130 M potentiostat, a high impedance millivoltmeter (Minisis 6000, Tacussel) and an X–Y recorder (IFELEC If 3802). Cyclic voltammetry, with scan rates ranging from 10 mV/s to 10 V/s, was carried out with an electrochemical device DACFAMOV equipped with an Apple II computer (Microtec, CNRS, Toulouse, France). The working electrode was a platinum disk (diameter 2 mm, type EDT, Tacussel), the auxiliary electrode was a platinum wire and the reference electrode was a saturated calomel electrode (SCE) connected to the studied solution by a bridge filled with $CH_2Cl_2 + 0.1$ *M* TBAP.

During preparative electrolysis, the anode and cathode compartments of the working cell were separated by a fritted glass disk. The working electrode was a platinum spiral wire (diameter 0.8 mm) 30 cm in length. The working potential was controlled by a PRT 100 potentiostat (Tacussel).

After each exhaustive electrolysis, the solution was concentrated under reduced pressure. Then pentane was added and the resulting precipitate was separated by filtration. This precipitate was treated with THF (in which TEAP is poorly soluble) and filtered through Celite. This allows the separation of TEAP as a solid. The filtered solution was then evaporated to dryness before further studies.

Preparation of $[(o\text{-}C_6H_4CH_2NMe_2)Pd\{Ph_2PCH_2C(O)(\eta^5\text{-}C_5H_4)Fe(\eta^5\text{-}C_5H_5)\}]\text{-}[ClO_4]([2\text{-}H][ClO_4])$

Complex **2** (0.100 g, 0.15 mmol) was electrolysed at 0.5 V/SCE in CH_2Cl_2 + TEAP (50 ml). Using the procedure described above for the work-up, [2-H][ClO_4] was isolated as a burgundy red powder (yield approx. 0.080 g). Anal. Found: C, 52.08; H, 4.35; N, 1.75. $C_{33}H_{33}ClNFeO_5PPd$ calc. (M_r = 752.31): C, 52.68; H, 4.42; N, 1.86%. IR(KBr): 1550 s (ν(CO)) cm^{-1}. UV-visible (CH_2Cl_2), λ_{max} (nm), ϵ (mol^{-1} dm^3 cm^{-1}): 498(2080), 358(3080), 290(sh). ^1H NMR ($CDCl_3$): δ 3.05 (d, 6H, NMe_2, $^4J(PH) = 2.4$ Hz); 4.00 (s, 5H, C_5H_5); 4.15 (d, 2H, NCH_2, $^4J(PH) = 1$ Hz); 4.41 (d, 2H, PCH_2, $^2J(PH) = 11.6$ Hz); 4.84 and 5.05 (two signals, AA′BB′ spin system, 4H, C_5H_4); 6.45–8.03 (14H, aromatic H). $^{31}P\{^1H\}$ NMR (C_6D_6/THF): δ 38.5 (s). The parent complex [2-H][PF_6] was prepared by reaction of **3** with 1 equiv. $TlPF_6$ in CH_2Cl_2. **CAUTION**: because of explosion risks, perchlorate salts are dangerous and should be avoided when possible.

Results and discussion

Electrochemical oxidation of $[Ph_2PCH_2C(O)(\eta^5\text{-}C_5H_4)Fe(\eta^5\text{-}C_5H_5)]$ *(1)*

With a rotating-disk electrode between 0 and +1.5 V/SCE, a single anodic voltammetric wave is observed at $E_{1/2} = 0.73 \pm 0.01$ V/SCE. The slope of 88 mV/unit log of the straight line plot of *E versus* $\log(I/I_d - I)$ indicates that the oxidation of **1** is not reversible. The limiting current, being proportional to $\omega^{1/2}$

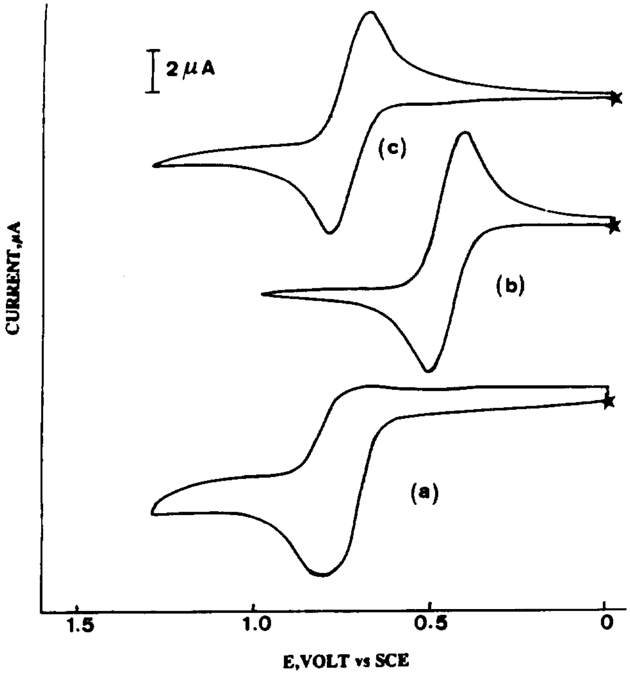

Fig. 1. Cyclic voltammograms in 0.1 *M* TBAP, CH_2Cl_2. (a) **1**, $c = 1.40 \times 10^{-3}$ *M*; (b) ferrocene, $c = 1.12 \times 10^{-3}$ *M*; (c) acetylferrocene, $c = 1.00 \times 10^{-3}$ *M*. * denotes start of the scan.

(ω = angular velocity) and to the concentration of **1**, indicates a diffusion controlled current obeying the LEVICH equation [4]. No reduction step was observed from 0 to −1.5 V/SCE.

Cyclic voltammograms exhibited only a well-defined anodic peak ($E_{pa} = 0.80 \pm 0.01$ V/SCE) at $v < 0.2$ V/s (Fig. 1(a)). This result contrasts with that observed for ferrocene (Fc) or acetylferrocene (Ac–Fc) for which the cyclic voltammograms display, respectively, two well-defined (one anodic and one cathodic) peaks (Fig. 1(b) and (c)). However, when the scan rate is increased ($v > 0.5$ V/s), a cathodic peak appears on the voltammogram (Fig. 2) which indicates that the oxidative process on the electrode may be associated with a subsequent chemical reaction. The plots of E_{pa} versus log v are linear, the values of $\partial E/\partial \log v$ over the scan rate range 0.02–5 V/s indicating that the chemical reaction is fast [5]. The ratio I_{pc}/I_{pa} increased from 0.5 to 0.97 when v increased from 0.5 to 5 V/s, showing that an irreversible chemical reaction follows the electron transfer. These results prompted us to check whether the ferrocenyl group was involved in the oxidation of **1**.

To this end, we studied by cyclic voltammetry the functionalized parent phosphine $Ph_2PCH_2C(O)(C_6H_4)$ (**1'**), derived from acetophenone. Over the entire scan rate range 0.02–5 V/s, we only observed a single, irreversible anodic peak ($E_{pa} = 1.5 \pm 0.01$ V/SCE). This strongly contrasts with the observations made for **1**, and therefore we conclude that the electrochemical oxidation of **1** at $E_{1/2} = 0.73$ V/SCE is likely to involve the ferrocenyl moiety.

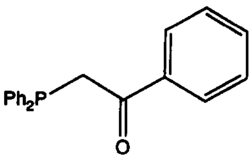

(1')

When exhaustive coulometry of **1** is carried out at the plateau potential ($E = 0.95$ V/SCE) of the oxidation stationary wave, two electrons are exchanged per mole of **1**. This result precludes oxidation of the ferrocenyl moiety in **1** alone at this potential, since such a process would only require a one-electron exchange.

The $I = f(t)$ reveals that the decrease of the current with time is not exponential and thus not under control of diffusion and electron transfer only, confirming the occurrence of a chemical reaction. The cathodic scan on a solution of **1** after oxidative electrolysis at 0.95 V/SCE shows two new waves (Fig. 3(b)), a mixed wave ($E_{1/2} = 0.8$ V/SCE) and another ill-defined, drawn-out cathodic signal around $E_{1/2} = 0.08$ V/SCE. The oxidation wave of the initial solution of **1** is given in Fig. 3(a) for comparison. The electronic absorption spectrum of the solution recorded immediately after oxidative electrolysis at 0.95 V/SCE contains a single absorption band ($\lambda = 231$ nm), and contrasts with the initial spectrum ($\lambda_1 = 462$ nm, $\lambda_2 = 340$ nm, $\lambda_3 = 235$ nm). Note also that the ESR spectrum of this fully electrochemically oxidized solution of **1**, recorded at 120 K under an inert atmo-

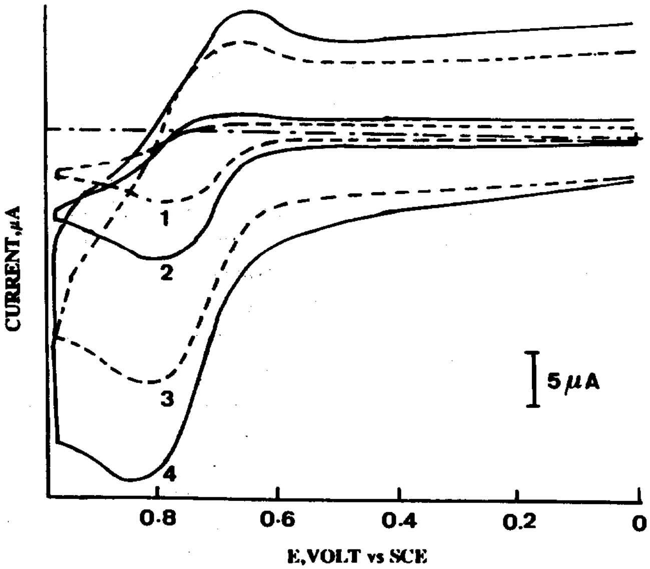

Fig. 2. Cyclic voltammograms of 5.33×10^{-4} M **1** in CH_2Cl_2, 0.1 M TBAP. Scan rates: (1) 0.1 V/s; (2) 0.5 V/s; (3) 1.0 V/s; (4) 2.0 V/s. * denotes start of the scan.

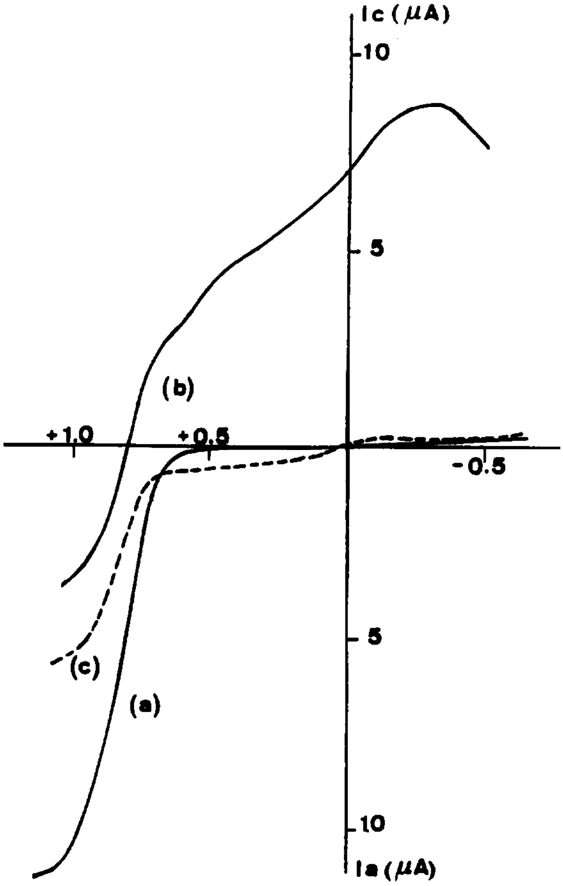

E,VOLT vs SCE

Fig. 3. Rotating disk voltammograms of 1.7×10^{-2} mmol **1** in CH_2Cl_2, 0.1 *M* TBAP ($N = 1000$ rev min^{-1}). (a) Before electrolysis; (b) after electrolysis at 0.95 V/SCE (two-electron exchange); (c) after electrolysis at 0.56 V/SCE (one-electron exchange).

sphere, shows two signals in the ranges 3000–3500 G and 1500–1700 G, with $\Delta H = 250$ G, $g = 2.0263$ and $\Delta H = 101$ G, $g = 4.253$, respectively. The ESR spectra obtained under the same conditions after electrolysis of ferrocene or acetylferrocene display a single signal between 1500 and 1700 G (Fc^+: $\Delta H = 100$ G, $g = 4.249$; $(Ac\text{–}Fc)^+$: $\Delta H = 100$ G, $g = 4.232$), similar to the signal at approximately 1600 G observed after oxidation of **1**; this implies that the ferrocenyl group is indeed involved in the oxidation of **1**. The second paramagnetic species in the solution of **1** at approximately 3250 G could not be identified. Note, however, that in a number of reports on ferricinium-derived ions, paramagnetic decomposition products have been described [6–10], and that significant decomposition of ferricinium cations may occur on the coulometric time-scale [11].

These results indicate that the two-electron exchange of **1** involves a ferrocene oxidation and also chemical(s) step(s) of which at least one seems to be a decomposition reaction.

One-electron oxidation of 1

When **1** was electrolysed at a constant potential corresponding to the beginning of the oxidation wave ($E = 0.60$ V/SCE) [12*], the number of electrons exchanged (n) is 1. A further cathodic scan on the oxidized solution from +1.2 to −1 V/SCE (Fig. 3(c)) shows an entirely anodic wave at $E_{1/2} = 0.80 \pm 0.01$ V/SCE (note that $I_{\text{lim}}(3a)/I_{\text{lim}}(3c) = 2$, as expected when only a single one-electron oxidation occurs). Cyclic voltammetry at 0.1 V/s on this oxidized solution exhibits a cathodic peak ($E_{\text{pc}} = 0.72$ V/SCE) and the associated anodic peak ($E_{\text{pa}} = 0.86$ V/SCE).

This one-electron oxidation was repeated on a preparative scale. After electrolysis, the solution was evaporated to dryness and the residue treated with THF. The resulting suspension was filtered through Celite, and the filtered solution evaporated. The ^{31}P NMR spectrum of the product obtained after work up clearly establishes that the phosphine has been completely transformed as a result of the electrochemical one-electron oxidation with further possible transformations during the work up (absence of the phosphine peak at $\delta = -19.1$ ppm (C_6D_6/THF)). This spectrum shows several peaks in the range 9–30 ppm, indicating that the electrochemical oxidation of **1** has induced chemical reaction(s) involving the phosphorus atom [13*]. These observations are in agreement with those recently reported by Pilloni *et al.* [14] on another ferrocene-derived phosphine, namely 1,1′-bis(diphenylphosphino)ferrocene (dppf).

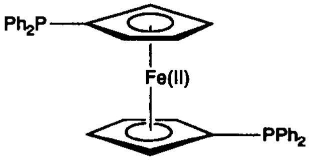

(dppf)

These authors observed that the one-electron oxidation of the ferrocene core in dppf is followed by a fast intramolecular electron transfer from one of the phosphorus atoms to the ferrocene moiety which then leads to a transient phosphonium-ferrocene radical species. It is noteworthy that the electronic absorption spectrum obtained immediately after the oxidative one-electron electrolysis of **1** is close to that of **1** and, in particular, the characteristic ferricinium band near 620 nm [15] is absent from this spectrum. Also, the ESR spectrum (120 K) of the solution obtained immediately after the one-electron oxidative electrolysis of **1** displays a very broad signal characterized with $\Delta H = 258$ G, $g = 2.011$, which may be attributed to a phosphonium radical cation [16].

Thus, the absence of a ferricinium cation in the solution, on the time-scale of macroscopic exhaustive oxidation of **1** and the simultaneous observation of new radicals indicate that the electro-generated ferricinium cations react with the phosphorus centre.

Scheme 1 summarizes this reaction path, which may be described as an $E_1C_1E_2C_2$ mechanism.

---

* Reference number with asterisk indicates a note in the list of references.

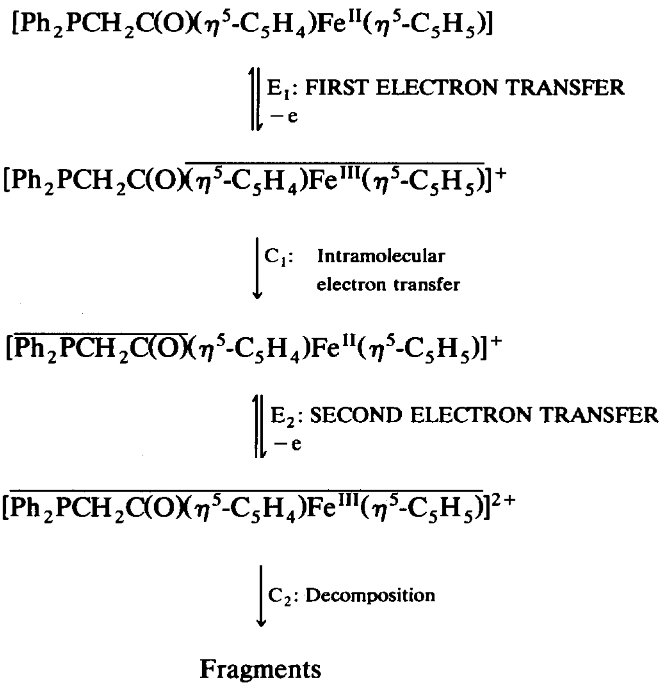

Scheme 1

It may be added that the homogeneous reaction C_1 is quite fast on the time-scale of the electrochemical methods. For instance, even spectroelectrochemical measurements after microcoulometric oxidation carried out at constant potential ($E = 0.60$ V/SCE) failed to detect the ferricinium band at 620 nm; the spectra obtained were then identical to those reported above for the solution resulting from the one-electron exhaustive electrooxidation of **1**. Consistent with this is the absence of any significant effect on the reversibility of cyclic voltammograms on lowering the temperature: for instance, within the scan rate range 0.01–0.1 V/s, the ratio I_{pc}/I_{pa} remains close to 0.5 even when the voltammograms are recorded at about −20°C instead of 25°C.

Electrochemical oxidation of $[(o\text{-}C_6H_4CH_2NMe_2)Pd\{Ph_2PCH{=}C(O)(\eta^5\text{-}C_5H_4)Fe(\eta^5\text{-}C_5H_5)\}]$ *(2) and* $[(o\text{-}C_6H_4CH_2NMe_2)PdCl\{Ph_2PCH_2C(O)(\eta^5\text{-}C_5H_4)Fe(\eta^5\text{-}C_5H_5)\}]$ *(3)*

Rotating disk electrode (RDE) voltammetry between 0 and 1.5 V/SCE revealed two oxidation steps for each of the two complexes. In both complexes, the first oxidation is reversible, whereas the second is irreversible. The limiting current, proportional to $\omega^{1/2}$ and to the concentration of the electroactive species, is a diffusion current which obeys the Levich equation [4]. The voltammetry characteristics are summarized in Table 1.

The comparison of the ${}^1E_{1/2}$ values with those usually observed in the same conditions with other substituted ferrocenes [17], with ferrocene, $E_{1/2} = 0.50 \pm 0.01$ V/SCE, with acetylferrocene, $E_{1/2} = 0.74 \pm 0.01$ V/SCE suggests that the first

Table 1

Rotating disk electrode voltammetry of the complexes **2** and **3**, in $CH_2Cl_2 + 0.1$ *M* TBAP

Species studied	Oxidation steps	$E_{1/2}$ (V/SCE) ± 0.01	log $I/I_d - I$ slope (mV/log)	Number of electron exchanged	Diffusion coefficient (10^6 cm^2 s^{-1})
2	1	0.47	66	1	3.2
	2	1.32	88	1	–
3	1	0.72	64	1	3.62
	2	1.40	117	1	–

electron-transfer involves the ferrocenyl redox centre. This hypothesis is consistent with the observed variation of $^1E_{1/2}$ to the electron-attracting acyl group in **3** and to the electron-donating enolate function in **2**.

In the parent palladium(II) complex $[(o\text{-}C_6H_4CH_2NMe_2)Pd(Ph_2PCH{=}C(O)Ph)]$ (**2′**) the only irreversible oxidation step measured was at $E_{1/2} = 1.22 \pm 0.01$ V/SCE. This result strongly supports the hypothesis that the first oxidation of **2** or **3** involves the ferrocenyl moiety. The second oxidation step may correspond to that of the palladium(II).

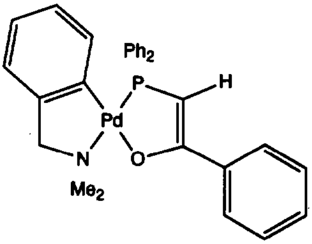

(**2'**)

The general shape of the cyclic voltammograms obtained in Fig. 4 shows two anodic peaks (1, 3) and two cathodic peaks (2, 4), all well-defined, plus one ill-defined, small anodic peak (5) located around 0.9–1.0 V/SCE. For the first oxidation step (peak 1), the peak current exhibits the characteristics of a diffusion-controlled current, *i.e.* the plots of I_{p_1} *versus* $v^{1/2}$ and *versus* c (c = concentration of the electroactive species) are linear over the scan rate range 0.02–0.5 V/s.

Over the same scan rate range, the change in the ratios I_{p_2}/I_{p_1} (0.87–0.97 for **2**, 0.66–0.91 for **3**) indicates that an irreversible chemical reaction follows the electron transfer [18]. This chemical reaction is faster in complex **3** than in **2**. In fact, at low scan rates ($v < 0.1$ V/s) the two peak currents 5 and 4 (complex **3**) are higher (Fig. 5(b)) than at faster scan rates (Fig. 4(b)). It is therefore reasonable that peak 5 should be due to the oxidation of an electroactive species generated by the chemical reaction which follows the first oxidation of **3** (peak 1).

As shown by these voltammograms, the first oxidation/reduction couple of peaks 1 and 2 exhibit a ΔE_p value characteristic of a quasi-reversible electron-transfer, namely a constant ΔE_p value 90 ± 10 mV at low and moderate scan rates ($v \leq 0.5$ V/s) and higher values of ΔE_p beyond 0.5 V/s.

If it is accepted that the first oxidation of **2** and **3** involves the ferrocenyl group, the above results are very consistent with the known characteristics of ferrocene

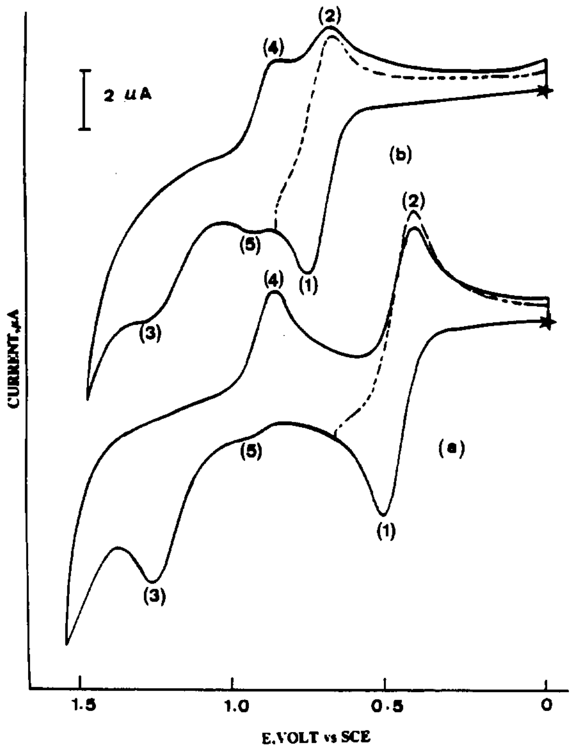

Fig. 4. Cyclic voltammograms of 7.16×10^{-4} *M* **2** (a) and 7.26×10^{-4} *M* **3** (b) in CH_2Cl_2, 0.1 *M* TBAP. Scan rate = 0.1 V/s. * denotes start of the scan.

and substituted ferrocenes [11,19–21] which oxidize quasi-reversibly in non-aqueous solvents. Recent results obtained on ultramicroelectrodes indicate that the actual electron-transfer rate is fast in the ferrocene/ferricinium interconversion [22].

The electrochemical oxidation of **2** and **3** was also monitored on a longer time-scale than cyclic voltammetry, by exhaustive coulometric electrolysis.

In the case of complex **2**, coulometry was carried out at $E = 0.65$ V/SCE for the first oxidation wave, for which $E_{1/2} = 0.47$ V/SCE (Fig. 6(a)). The number of electrons exchanged (n) is 1. The cathodic scan of the solution obtained (Fig. 6(b)) shows, as expected, a cathodic wave with a half-wave potential of $E_{1/2} = 0.45 \pm 0.01$ V/SCE. However, the height of the wave (Fig. 6(b)) is markedly smaller than theoretically expected, and this observation is consistent with the occurrence of the chemical reaction detected in cyclic voltammetry. Several minutes (10–15 min) after this coulometry at 0.65 V/SCE was completed, the wave shown in Fig. 6(b) disappeared, and two new waves (Fig. 6(c)) were observed: one of these waves around 0.90 V/SCE was composite and totally anodic, the other was cathodic and ill-defined ($E_{1/2} = -0.3$ V/SCE). Finally, 30–45 min after the end of the electrolysis, only the anodic wave around 0.9 V/SCE (Fig. 6(c)) remained observable. Furthermore, after this oxidative coulometry at 0.65 V/SCE, the wave corresponding to the second oxidation step (Table 1), assigned to the Pd^{II}-containing moiety, was no longer observable.

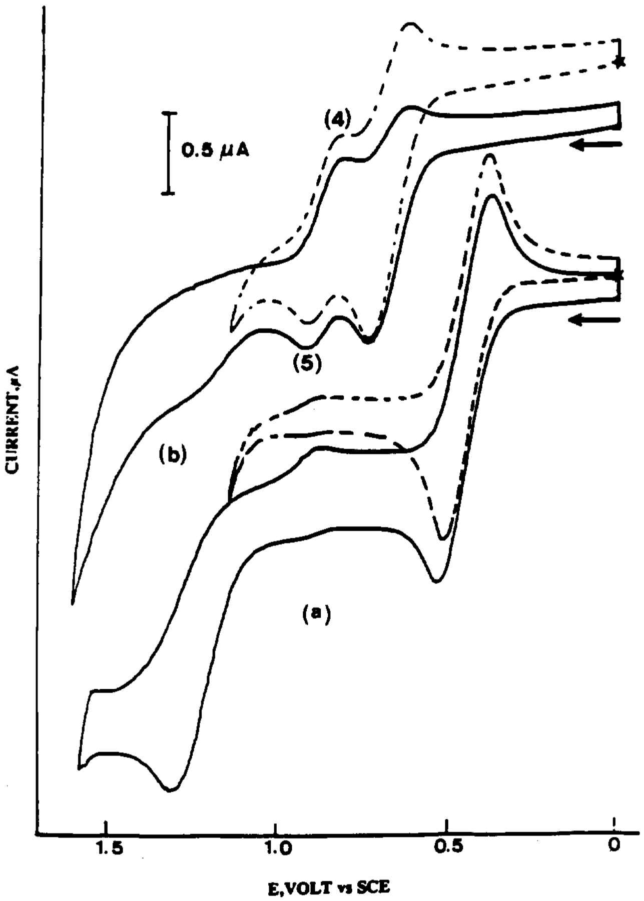

Fig. 5. Cyclic voltammograms of 7.16×10^{-4} *M* **2** (a) and 7.26×10^{-4} *M* **3** (b) in CH_2Cl_2, 0.1 *M* TBAP. Scan rate = 0.01 V/s. * denotes start of the scan from 0 to +1.2 V/SCE.

It is noteworthy that the electronic spectrum measured at this stage of the observed transformations displays no band in the range characteristic of ferricinium complexes [23–26]. Note also that the ESR spectrum (120 K) of the electrolysed solution shows a signal typical of a radical cation ($\Delta H = 16.7$ G, $g = 2.008$). Although not assignable, this signal is distinct from that expected for the Fc^+ or $(Ac–Fc)^+$ species. These results are consistent with an electron-transfer from the palladium-metallocyclic unit to the ferricinium moiety in the primary oxidation product of **2**.

We carried out preparative coulometry on 100 mg of **2** with the aim of identifying the final oxidation product. The potential was set at 0.5 V/SCE [27*]. After work up (see Experimental section), we isolated a reddish-violet compound (80 mg) which was identified as $[2\text{-H}][ClO_4]$. This complex contains a chelating phosphine-ketone ligand.

The oxidation potential ($E_{1/2} = 0.92 \pm 0.01$ V/SCE) of an authentic sample of $[2\text{-H}][PF_6]$ (see Experimental section) was also measured and found very close to

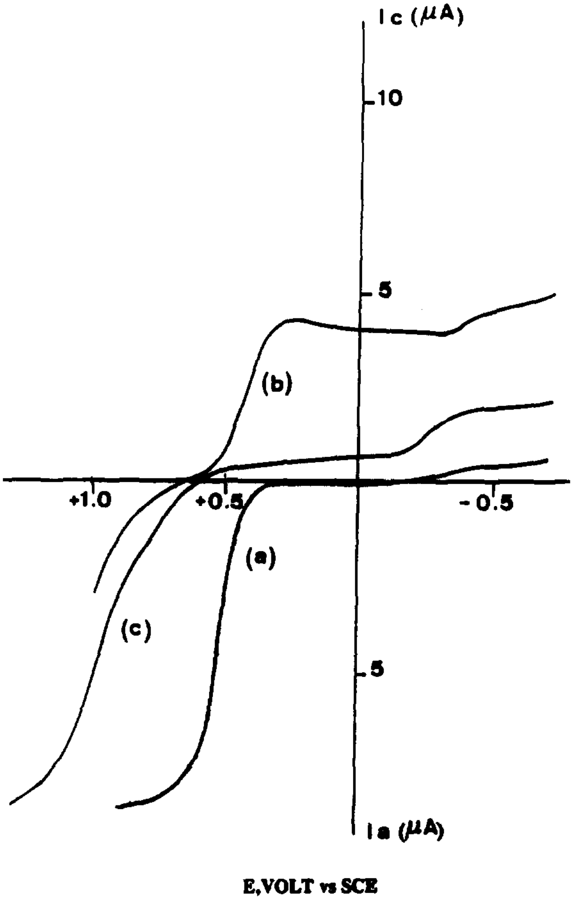

Fig. 6. Voltammograms at a RDE of 1.7×10^{-2} mmol 2 in CH_2Cl_2, 0.1 *M* TBAP ($N = 1000$ rev min^{-1}) obtained before electrolysis (a), after electrolysis at 0.65 V/SCE (b) and 20 min later (c).

that of the species resulting from the one-electron exhaustive electrooxidation of **2** (Fig. 6(c)).

The above results lead to the conclusion that the one-electron oxidation of **2** triggers the formation of a reactive radical cation, which, once formed, easily undergoes hydrogenation, *e.g.* by reaction with the solvent, to give the stable cationic complex [2-H][ClO_4].

For complex **3** the situation is somewhat different. Exhaustive electrolysis of **3** at the plateau potential of the first oxidation wave ($E = 0.95$ V/SCE) indicates that $n = 1.7$. This value deserves further analysis since it is not an integer and furthermore it varies between the limits $1 < n < 1.65$ with the electrolysis potential between 0.65 and 0.85 V/SCE: the value of n increases with applied potential. In order to explain this, we carried out the electrolysis at a potential corresponding to the passage of one Faraday per mole of **3** (E_{applied} slightly above 0.6 V/SCE). The cathodic scan, from +1.2 to −1 V/SCE, of the resulting solution (Fig. 7(b)) does not show the expected reduction wave that would correspond to a reversible one-electron transfer but displays a totally anodic wave at about $E_{1/2} = 0.90 \pm 0.01$

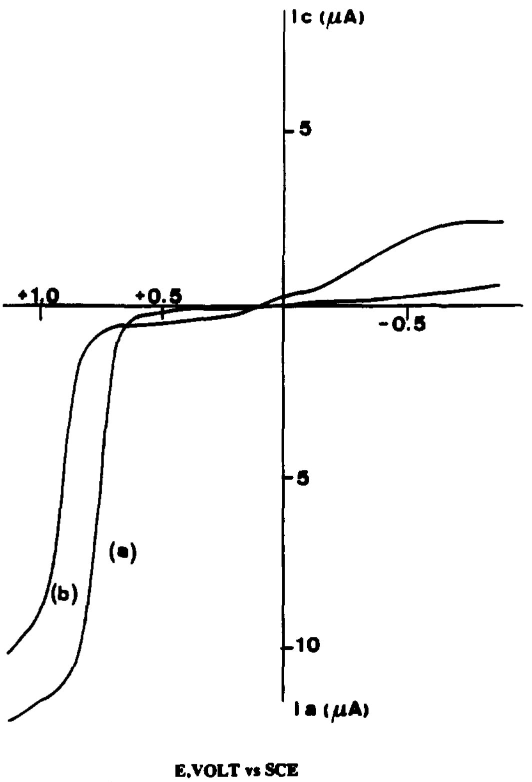

Fig. 7. Voltammograms at a RDE of 1.69×10^{-2} mmol 3 in CH_2Cl_2, 0.1 *M* TBAP ($N = 1000$ rev min^{-1}). (a) Before electrolysis; (b) after consumption of one electron per molecule at the applied potential 0.65 V/SCE.

V/SCE and a broad cathodic wave at $E_{1/2} = -0.3$ V/SCE. These results confirm the occurrence of the chemical reaction inferred from cyclic voltammetry and indicate that the anodic oxidation of 3 generates electroactive species of which at least one is very stable and further oxidizable at $E_{1/2} = 0.90$ V/SCE. The potential difference (~ 180 mV) between the oxidation wave ($E_{1/2} = 0.90$ V/SCE (Fig. 7(b)) of this new species and that of complex 3 (Table 1 and Fig. 7(a)) shows that, unless the electrochemical oxidation of 3 is carried out at a potential less than about +0.7 V/SCE, the exhaustive electrooxidation of 3 involves additionally the oxidation of the species generated (Fig. 7(b)), thus giving $n > 1$. The other species characterized by its half-wave potential $E_{1/2} = -0.3$ V/SCE is not chemically stable and its reduction wave changes with time, becoming more and more ill-defined, whilst I_{lim} decreases. It should be noted that an analogue cathodic wave was already observed in the case of complex 2 but only several minutes after the completion of electrolysis (Fig. 6(c)). Furthermore, as for complex 2, after oxidative electrolysis at 0.6–0.7 V/SCE, the oxidation step corresponding to the second oxidation of 3 (peak 3 in Fig. 4(b)) has disappeared. These results confirm that the chemical reaction following the first oxidative electron transfer is faster in complex 3 than in 2, and that it produces a stable species oxidizable at $E_{1/2} = 0.90$ V/SCE and a transient species reducible around $E_{1/2} = -0.3$ V/SCE.

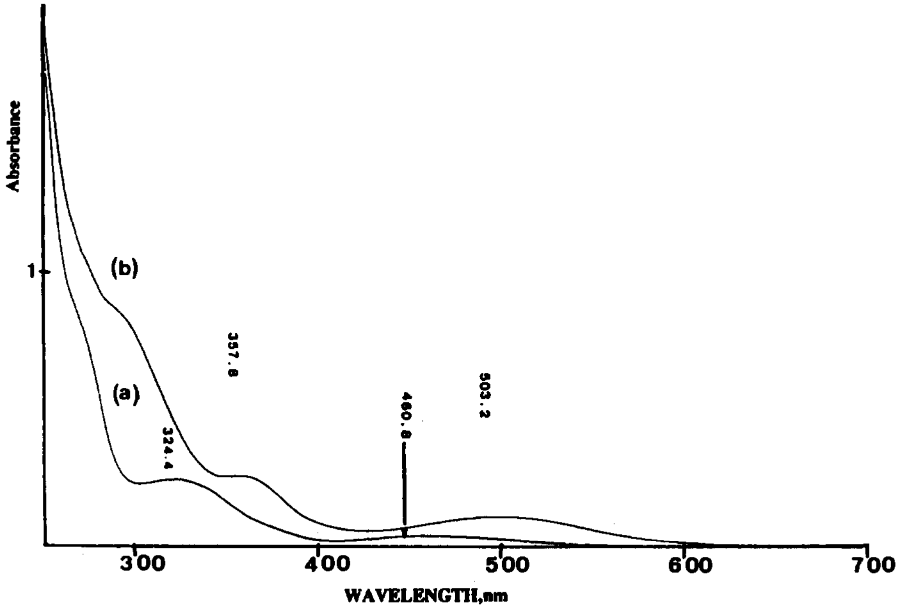

Fig. 8. Electronic absorption spectra of 3 (a) and 3^+ (b) in CH_2Cl_2.

In the solution obtained after the one-electron oxidative electrolysis of 3, the ^{31}P NMR spectrum and the electronic absorption spectrum (Fig. 8) revealed the presence, among other species, of the cation $(2\text{-H})^+$ (absorption bands at 503 nm, 358 nm and 290(sh) nm). Bands at $\lambda \approx 500$ nm, 290(sh) nm were also observed in the solution obtained after exhaustive one-electron oxidation of 2. These results may be interpreted in terms of an electron-transfer from palladium to the ferricinium moiety with subsequent loss of chlorine (Scheme 2) and stabilization of the resulting cation by formation of the chelate complex [2-H][ClO_4]. This complex may also arise by loss of HCl and formation of $C^{\cdot +}$ (Scheme 2). This mechanism is in agreement with the ESR measurements which revealed identical signals for electrolysed (one-electron oxidation) solutions of both 2 and 3.

In summary, the above electrochemical results obtained with complexes 2 and 3 demonstrate the occurrence of an irreversible reaction after the first oxidative electron transfer. This reaction generates two electroactive species: a relatively unstable electro-reducible one ($E_{1/2} = -0.3$ V/SCE) and an electrooxidizable one, characterized as [2-H][ClO_4].

The above results indicate that initial one-electron oxidation of 2 or 3 corresponds to the conversion of Fc to Fc^+ in these molecules. It has been shown by others that the ferricinium ion may act as an oxidant (internal redox mediator) in indirect electrochemical oxidation reactions [28–30]. This may operate here, with Pd^{II} oxidized to unstable Pd^{III}, the electron transfer occurring through the β-ketophosphine. However, the intramolecular oxidation of the Pd^{II} by a ferricinium centre is thermodynamically unfavourable: the Pd^{II} centre is oxidized irreversibly at +1.22 V/SCE (species 2′) in the absence of the linked ferrocenyl group, whereas the oxidation of the ferrocenyl group takes place at +0.47 V/SCE in 2 and at +0.72 V/SCE in 3. The internal redox oxidation, in 2^+ or 3^+, of the Pd^{II} by the coordinated ferricinium is nevertheless possible on the following grounds:

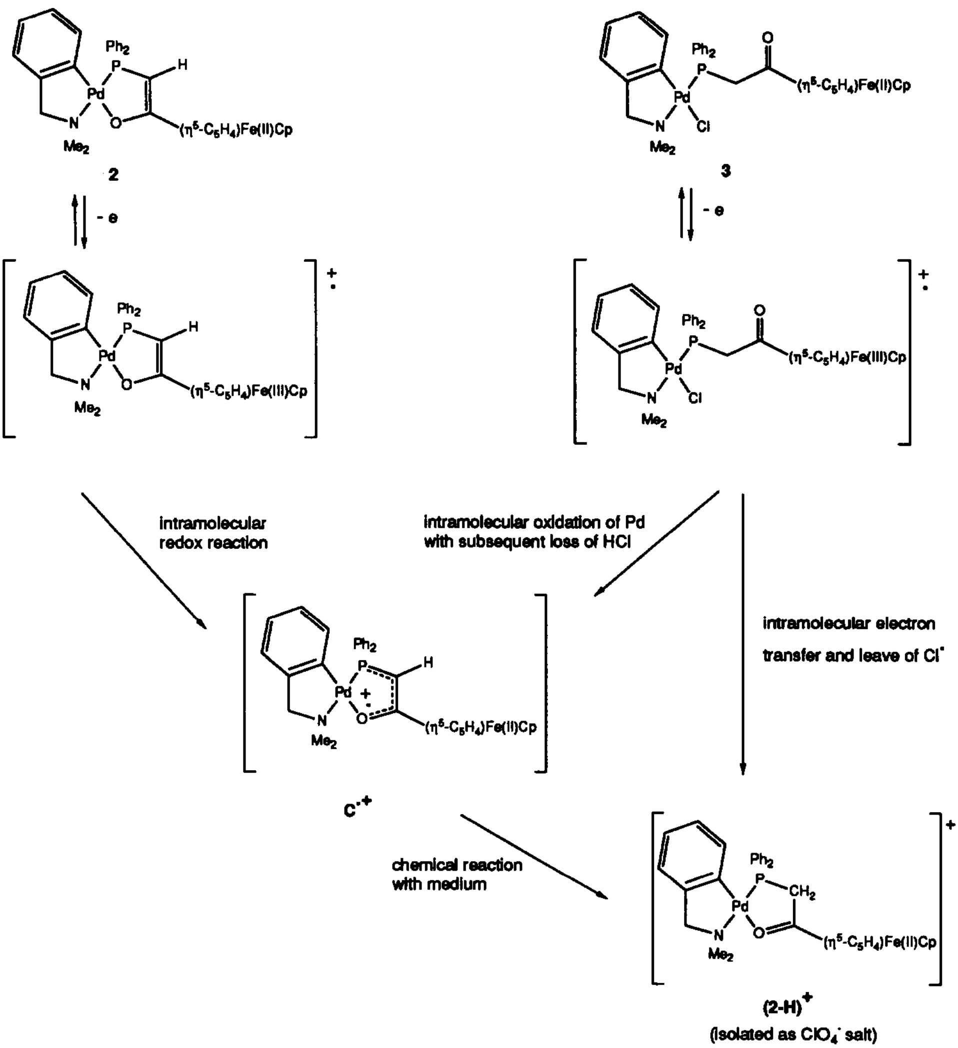

Scheme 2.

(a) the ferrocenyl group is a powerful inductive electron donor [31,32]. This should make the oxidation of the Pd^{II} moiety much easier.

(b) Furthermore, the oxidized acetylferrocene, $[\{H_3CC(O)(C_5H_4)\}Fe^{III}(C_5H_5)]^+$ ($E_{1/2} = 0.74$ V/SCE), does not oxidize 2′. This strongly suggests that electron-transfer between palladium(II) and the ferricinium moieties observed in molecules 2^+ and 3^+ occurs through an intramolecular mechanism favoured by the conjugated enolate function.

The results reported and discussed above are summarized in Scheme 2.

Concluding remarks

The present study establishes that the oxidations of **1** and **3** are close to that of acetylferrocene, whereas the oxidation of the enolate **2** compares with that of ferrocene. This behaviour may be attributed to the electron-withdrawing ketone groups in **1**, **3** and Ac–Fc, and to the electron-donating character of the enolate in **2**, respectively.

The oxidation of the ferrocenyl centres of **1**, **2** and **3** is followed by an intramolecular electron-transfer leading ultimately to cationic Fe^{II} species which contain transient phosphorus- or palladium-centred radical cations. We are currently investigating the possibility of stabilizing such radicals. Further studies will concern the use of the ferrocenyl phosphine **1** as internal redox mediator, to discover new bimetallic systems allowing electronic communication.

References and notes

1 See for example: (a) D.A. Wrobleski and T.B. Rauchfuss, J. Am. Chem. Soc., 104 (1982) 2314; (b) D.A. Wrobleski, C.S. Day, B.A. Goodman and T.B. Rauchfuss, J. Am. Chem. Soc., 106 (1984) 5464; (c) A.W. Maverick, S.C. Buckingham, Q. Yao, J.R. Bradbury and G. Stanley, J. Am. Chem. Soc., 108 (1986) 7430.
2 See for example: (a) O. Kahn, Structure and Bonding, Vol. 68, Springer, Berlin, 1987, p. 89; (b) G.A. Fox and C.G. Pierpont, J. Chem. Soc., Chem. Commun., (1988) 806.
3 P. Braunstein, T.M. Gomes Carneiro, D. Matt, F. Balegroune and D. Grandjean, J. Organomet. Chem., 367 (1989) 117.
4 V.G. Levich, Physico-Chemical Hydrodynamics, Prentice Hall, Englewood Cliffs, NJ, 1962.
5 L. Nadjo and J.M. Saveant, J. Electroanal. Chem., Interfacial Electrochem., 48 (1973) 113.
6 A. Horsfield and A. Wassermann, J. Chem. Soc. A, (1979) 3202.
7 A. Horsfield and A. Wassermann, J. Chem. Soc., Dalton Trans., (1972) 187.
8 R. Prins and F.J. Reinders, J. Am. Chem. Soc., 91 (1969) 4229.
9 R. Prins, Mol. Phys., 19 (1970) 603.
10 R. Aasa, J. Chem. Phys., 52 (1970) 3919.
11 J.W. Diggle and A.J. Parker, Electrochim. Acta, 18 (1973) 975.
12 Assuming that the oxidation wave at $E_{1/2} = 0.73$ V/SCE is composite, this potential was selected so that the oxidation of **1** only affects the first step, *i.e.* the ferrocenyl group.
13 Among the formed species, traces of oxide [1-(O)] were unambiguously identified by comparison (UV and voltammetric results) with an authentic sample.
14 G. Pilloni, B. Longato and B. Corain, J. Organomet. Chem., 420 (1991) 57.
15 S.B. Colbran, B.H. Robinson and J. Simpson, Organometallics, 2 (1983) 943, 952.
16 G.W. Eastland and M.C.R. Symons, J. Chem. Soc., Perkin Trans. 2, (1977) 833.
17 J.C. Kotz, in A.J. Fry and W.E. Britton (Eds.), Topics in Organic Electrochemistry, Plenum, New York, 1986, Chap. 3.
18 R.S. Nicholson and I. Shain, Anal. Chem., 36 (1964) 706.
19 U. Löffler, W. Göpel and B. Speiser, Electroanalysis, 3 (1991) 917.
20 S.U.M. Khan, J. Chem. Soc., Faraday Trans. 1, 85(8) (1989) 2001.
21 N.R. Armstrong, R.K. Quinn and N.E. Vanderborgh, J. Electrochem. Soc., 123(5) (1976) 646.
22 A.S. Baranski, K. Winkler and W.R. Fawcett, J. Electroanal. Chem., 313 (1991) 367.
23 R. Prins, Chem. Commun., (1970) 280.
24 R.H. Maki and T.E. Berry, J. Am. Chem. Soc., 87 (1965) 44437.
25 D.N. Hendrickson, Y.S. Sohn and H.B. Gray, Inorg. Chem., 10 (1971) 1559.
26 J.C. Kotz, E.E. Getty and L. Lin, Organometallics, 4 (1985) 610.
27 This potential was selected after several electrolyses at different potentials, which showed that the internal redox conversion of the primary oxidation product of **2** is slow. This conversion is quantitative for an electrolysis potential taken at the beginning of the oxidation wave, with, however, no further oxidation of the conversion product at this potential.
28 C. Degrand, A. Radecki-Sudre and J. Besançon, Organometallics, 1 (1982) 1311.
29 C. Degrand, A. Radecki-Sudre and J. Besançon, J. Electroanal. Chem., Interfacial Electrochem., 160 (1984) 199.
30 C. Degrand and A. Radecki-Sudre, J. Organomet. Chem., 268 (1984) 63.
31 J.A. Connor, E.M. Jones and J.P. Lloyd, J. Organomet. Chem., 24 (1970) C20.
32 J.A. Connor and J.P. Lloyd, J. Chem. Soc., Dalton Trans., (1972) 1470.